

The chemical composition of uraninite in Variscan granites of the Erzgebirge, Germany¹

H.-J. FÖRSTER

GeoForschungsZentrum Potsdam, Telegrafenberg, D - 14473 Potsdam, Germany

ABSTRACT

Uraninite is widespread as an accessory mineral in the Erzgebirge granites. It occurs throughout the entire comagmatic series of strongly peraluminous S-type Li-mica granites and has been discovered in more evolved transitional I-S type biotite and two-mica granites, but is rare in those of A-type affinity. Textural relationships and chemical ages imply that uraninite is of magmatic origin. Its composition is variable with a proportion of U plus radiogenic Pb between 71 and 99 mol.%. Uraninite has incorporated Th, Y, and the REE in total amounts between 1 and 29 mol.%. Elements such as P, Si, Al, Ca, and Fe are subordinate. Uraninite from two-mica and Li-mica granites is low in ThO₂ (0.8–6.5 wt.%), Y₂O₃ (0–0.8 wt.%) and REE₂O₃ (0.1–0.6 wt.%). In contrast, biotite granites from the Kirchberg pluton contain uraninite which is enriched in these components (in wt.%) (ThO₂ = 5.6–11.0, Y₂O₃ = 0.6–5.5, Ce₂O₃ = 0.1–0.6, Dy₂O₃ = 0.2–1.1). Commonly, the lanthanide and actinide contents in uraninite correlate poorly with those in the host granite. In S-type Li-mica granites as well as fractionated two-mica and biotite granites, uraninite is the dominant contributor to the bulk-rock U content. Here the proportion of U approaches 80–90%.

KEYWORDS: uraninite, composition, accessory minerals, granites, electron microprobe.

Introduction

ACCESSORY minerals constitute the major hosts of lanthanides (except Eu) and yttrium, actinides and other high field-strength elements (Zr, Hf, Nb, Ta, etc.) in granitic and other crustal rocks.

In peraluminous granites, a considerable portion of the bulk-rock uranium content may be ascribed to magmatic UO₂ (uraninite). In strongly peraluminous low-Ca granites, uraninite may host up to 90% of the bulk-rock uranium, but only insignificant portions of the thorium concentrations which are predominantly controlled by monazite-group minerals (Friedrich and Cuney, 1989).

Although having a great potential for radiogenic age dating, uraninite of magmatic or pegmatitic origin is rarely used in conventional

U-Pb geochronology (e.g. Rimsaite, 1989). On the other hand, uraninite was frequently used successfully for determining chemical U-Pb ages in granitic rocks (e.g. Snetsinger and Polkowski, 1977; Basham *et al.*, 1982; Cuney *et al.*, 1984; Jefferies, 1985; Charoy, 1986; Kucha *et al.*, 1986; Bowles, 1990 and references therein, Leupolt, 1992), anatectites (Parslow *et al.*, 1985), and U deposits (Kotzer and Kyser, 1993; Fayek *et al.*, 1997).

The crystal chemistry of uraninite from granitic rocks and related pegmatites, as analysed by electron microprobe, was the subject of numerous papers mostly published in the '80s (Snetsinger and Polkowski, 1977; Basham *et al.*, 1982; Cuney *et al.*, 1984; Chauris *et al.*, 1985; Jefferies, 1985; Charoy, 1986; Poty *et al.*, 1986; Feely *et al.*, 1989; Rong *et al.*, 1989; Thorpe *et al.*, 1990; Leupolt, 1992; Yudinsev and Simonova, 1992; Bea, 1996). Microprobe data on uraninite from metamorphic environments are rare (Rimsaite, 1989; Chernyshev and Golubev, 1996), and mineral compositions reported from uranium

¹ This paper is Part III of a series on REE-Y-Th-U-rich accessory minerals in peraluminous granites.

ores most commonly refer to its low-temperature variety pitchblende.

Most studies of uraninite composition have the disadvantage that they report either the concentration ranges for specific elements only, or list a single or a few individual analyses which include only a limited spectrum of the elements (U + Th + Pb \pm Y \pm Ce) actually present in the mineral in concentrations above the microprobe sensitivity. In particular the capability of uraninite for substituting the lanthanides is poorly understood. More complete analyses of uraninites including data for the light (*LREE*) and heavy rare-earth elements (*HREE*) obtained by electron microprobe are rare (Feely *et al.*, 1989; Bea, 1996), as are analyses performed by instrumental neutron activation analysis (INAA; Fryer and Taylor, 1987), inductively coupled plasma-mass spectrometry (ICP-MS; Hidaka *et al.*, 1992), and laser ablation inductively coupled plasma-mass spectrometry (LA-ICP-MS; Jackson *et al.*, 1992; Foord *et al.*, 1997).

In the past, uraninite abundance was mainly used as a tool in evaluating the uranium fertility of granitic rocks. It has been demonstrated that peraluminous granites rich in uraninite are the major source of uranium that occurs in pitchblende veins in the granite margins and country rocks (Basham *et al.*, 1982; Cuney and Friedrich, 1987; Tischendorf and Förster, 1994). Stability, and hence leachability of uraninite is critically dependent on its ThO₂ content (Grandstaff, 1976; cited in Pagel, 1982a). Economic U mineralization is commonly spatially related to U-rich leucogranites containing Th-poor uraninite which is highly soluble under hydrothermal and supergene conditions (Poty *et al.*, 1986).

Although the Variscan Erzgebirge/Krušné hory (Germany/Czech Republic) is distinguished by the frequent occurrence of granites strongly enriched in uranium (20 to 40 ppm in unaltered samples) and constitutes one of the major uranium provinces in Europe (e.g. Lange *et al.*, 1991), surprisingly, the presence of uraninite was recognized in only a few granites (see section on occurrences of uraninite-bearing granites) and was considered to be unusual rather than commonplace. Uraninite U-Th-total Pb data were reported only once, for a single grain from the Eibenstock granite (Yudintsev and Simonova, 1992).

Given their U enrichment, most of the Erzgebirge granites must contain magmatic uraninite. Therefore, a systematic mineralogical

investigation should help establish new occurrences of uraninite in this region. Furthermore, compositional heterogeneity of these peraluminous granites (Förster and Tischendorf, 1994; Förster *et al.*, 1995) is considered as favourable for discovering uraninite which might be variable in terms of actinide and lanthanide element contents. This paper reports and discusses the composition of uraninite gained from a comprehensive electron microprobe study of *REE*-Y-Th-U-rich accessories from mildly to strongly peraluminous granites of the Variscan Erzgebirge province. Similar to the previous papers on monazite-group minerals (Förster, 1998a) and xenotime (Förster, 1998b), special emphasis is placed on the compositional diversity of uraninite in relation to the host rock geochemistry. Consequently, the results are shown separately for the three major groups of granitic rocks, in which the mineral was identified during this study: [1] biotite granites, [2] two-mica granites, and [3] S-type Li-mica granites. Owing to its range of differentiation, which is greatest compared with those of other uraninite-bearing granite massifs in the region, the multiphase weakly peraluminous Kirchberg granite pluton (A/CNK = 1.05–1.09) was selected to investigate the evolution of uraninite chemistry in the course of biotite-granite fractionation. The mineral was further included in mass-balance calculations, which are still in progress, to obtain reliable quantitative information on its contribution to the whole-rock actinide and lanthanide contents. The compositional data are finally compared to uraninite compositions worldwide to get a closer insight into the overall chemical variability of uraninite in granitic rocks.

The results also have important implications for the crucial role of granites in the genesis of the perigranitic U mineralization in the Erzgebirge metallogenic province, specifically for explaining from a mineralogical point of view the observed regional distribution of U deposits in relation to fertile and non-productive granitic rocks. A detailed discussion of this subject, based on the integration of bulk-rock geochemical, geochronological and geological evidence is beyond the scope of this paper and will be made in a forthcoming article (Förster *et al.*, in prep.).

Analytical procedure

Uraninite was analysed for P, Si, Th, U, *REE* (except Eu and Tm and, in most cases, Ho and

Lu), Y, Al, Fe, Ca, and Pb with an automated CAMEBAX SX-50 electron microprobe at the GFZ Potsdam using wavelength-dispersive techniques. The operating conditions were as follows: accelerating voltage 20 kV, beam current 40–60 nA, and beam diameter 1–2 μm .

K α -lines were used for P, Si, Fe, Ca, and F; L α -lines for Y, La, Ce, Yb and Lu; and L β -lines for Pr, Nd, Sm, Gd, Tb, Dy, Ho and Er. Primary standards included pure metals for Th and U (also synthetic UO_{2.15}), vanadinite and a synthetic glass (0.79 wt.% PbO) for Pb, synthetic phosphates prepared by Jarosewich and Boatner (1991) for the REE, and natural minerals and synthetic oxides for other elements. The calibration was checked routinely using the synthetic glass SRM 610, which contains low contents of Th, U, and Pb, and the REE glasses prepared by Drake and Weill (1972). Counting times, data reduction, analysing crystals, analytical precision, and detection limits are described in detail in Förster (1998a).

Elements including Nb, Ta, Ti, Zr, and Na, which are occasionally reported in uraninite from granite in concentrations of some 100 ppm to a few thousand ppm (e.g. Bea, 1996), were not sought.

Back-scattered electron imaging (BSE) confirmed that the spot analyses were conducted within compositionally homogeneous areas. Therefore, the presence of mineral inclusions as contaminants can be ruled out within the BSE resolution of the machine.

REE, Y, Th, and U determinations in the whole-rock were performed by ICP-MS as described by Förster (1998a). The major elements were analysed by wavelength-dispersion X-ray fluorescence spectrometry.

Occurrences of uraninite-bearing granites in the Erzgebirge

The geology of the Variscan Erzgebirge and specifically the geochemistry and mineralogy of the granitic rocks has been described in the past in numerous publications (see Tischendorf, 1989). The following gives a brief summary.

In the late Carboniferous and early Permian, the Erzgebirge crust was invaded by rhyodacitic-rhyolitic lava flows and dikes and, more significantly in volume, intruded by granitic plutons of highly variable, usually evolved compositions (Fig. 1). The late- to post-collisional granites typically form composite bodies built up

by a succession of texturally and compositionally distinct, mapable sub-intrusions (Förster and Tischendorf, 1994). The latest intrusions and aplitic dikes reach extreme degrees of magma differentiation, often coupled with late-magmatic overprinting by residual fluids, which altered the magmatic minerals and disturbed the initial chemical composition of the bulk rock.

The granitic rocks are grouped into five main types [1] through [5] based on geological, mineralogical, and geochemical criteria (Förster *et al.*, 1998) and are listed below. Prior to completion of this study, uraninite has only been identified from four discrete occurrences, the S-type Ehrenfriedersdorf (Thomas, 1988) and Eibenstock Li-mica granites (Yudintsev and Simonova, 1992), and the A-type low-phosphorus Li-mica granites of Schellerhau (H. Bräuer, pers. comm.) and of Cinovec/Zinnwald (Cocherie *et al.*, 1991). These, and the newly established occurrences are given in parentheses and are shown in Fig. 1:

- [1] transitional I-S type low-fluorine biotite granites with muscovite-bearing aplites (Kirchberg, Burkersdorf, Schlema-Alberoda, Bernsbach, Beierfeld, Niederbobritzsch);
- [2] transitional I-S type low-fluorine two-mica granites with tourmaline-muscovite aplites (Bergen, Lauter, Schwarzenberg);
- [3] S-type high-fluorine, high-phosphorus Li-mica granites (Eibenstock, Tellerhäuser, Satzung, Pobershau);
- [4] aluminous A-type high-fluorine, low-phosphorus Li-mica granites (Schellerhau, Zinnwald);
- [5] aluminous A-type high-fluorine, low-phosphorus biotite granites.

Petrographic description of uraninite and assemblages of radioactive accessory minerals

Uraninite in the amphibole-lacking biotite granites is accompanied by apatite, zircon, monazite, solid solutions of thorite-zircon, thorite-coffinite (uranothorite), and thorite-xenotime and, specifically in the aplites within the Kirchberg massif, by rare cheralite-(Ce) and huttonitic monazite-(Ce). It has an average frequency of occurrence of 1–3 crystals per thin-section. Uraninite has not been observed in granites which contain allanite-(Ce) instead of monazite-(Ce), but may be present in small amounts.

The radioactive accessory mineral associations in two-mica and S-type Li-mica granites are less complex and comprise apatite, zircon, xenotime,

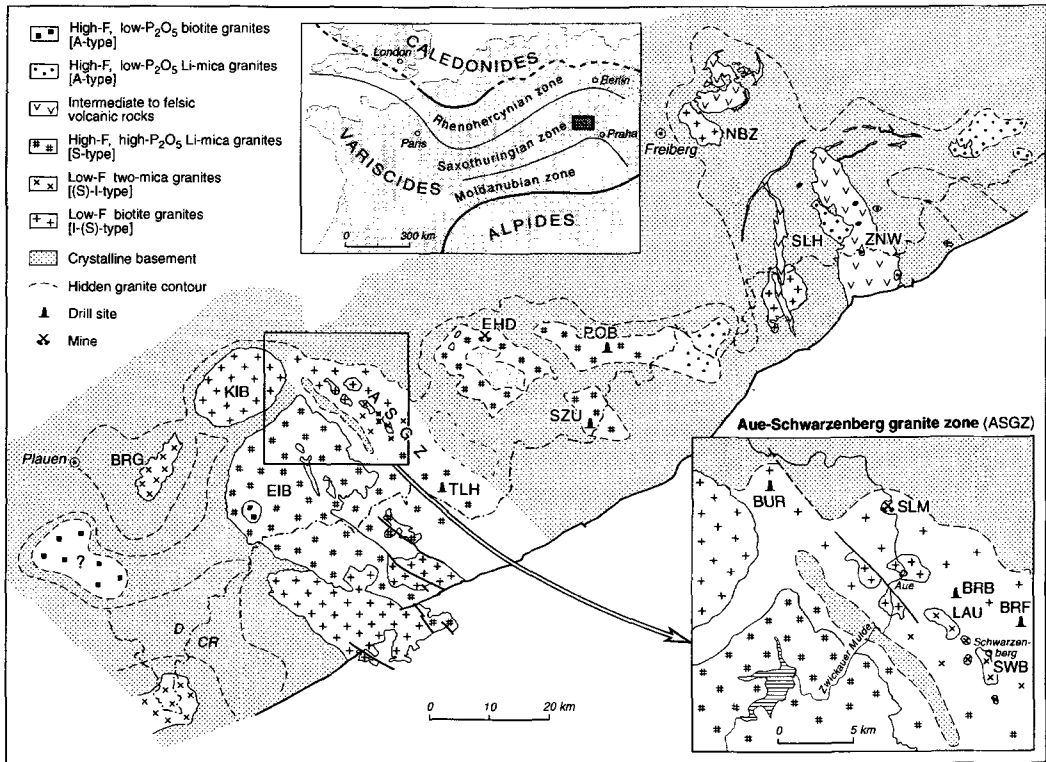


FIG. 1. Geological map, showing the regional distribution of the different groups of Variscan granites in the Erzgebirge (slightly modified from Förster *et al.* 1998). Uraninite-bearing granites are abbreviated as follows: BRG - Bergen, EIB - Eibenstock, KIB - Kirchberg, BUR - Burknersdorf, SLM - Schlema-Alberoda, BRB - Bernsbach, BRF - Beierfeld, LAU - Lauter, SWB - Schwarzenberg, TLH - Tellerhäuser, EHD - Ehrenfriedersdorf, POB - Pobershau, SLH - Schellerhau, ZNW - Zinnwald (Cinovec). The dash-dot line marks the border between Germany (D) and the Czech Republic (CR).

and minerals of the monazite group including cheralite-(Ce) and brabantite (Förster, 1998a). Uraninite is present throughout the entire series of comagmatic granites within composite Li-mica granite plutons. It also occurs in evolved two-mica granites. Its frequency is proportional to the U content of the sample and ranges from approximately 5 to more than 20 grains per thin-section.

The petrography and textural relationships of uraninite in the Erzgebirge granites (Figs. 2a–f) is similar to uraninite described from others in the Variscides of Europe (e.g. Basham *et al.*, 1982; Jefferies, 1985; Poty *et al.*, 1986). It occurs typically as euhedral to subhedral, solitary crystals of cubo-octahedral form and grain sizes between 5 and 30 μm . The complete range is from less than 2 to more than 200 μm across. Uraninite

may be hosted by all major minerals of the granite including trioctahedral micas, quartz, plagioclase, and K-feldspar. It has generated radioactive damage zones particularly in trioctahedral mica, feldspar and at grain boundaries, in which pyrite, Fe oxides and other late minerals have precipitated. Uraninite is occasionally associated with rutile and zircon and forms intergrowths with monazite. Rarely, it also forms minute inclusions in rutile as well as thin exsolutions in zircon and xenotime, the grain size of which does not permit accurate analysis. Euhedral uraninite with overall well-defined crystal faces is restricted to the freshest granite samples. It is subordinate in relative abundance to grains displaying variable degrees of surface dissolution. Compositionally quasi-homogeneous uraninite largely predomi-

CHEMICAL COMPOSITION OF URANINITE

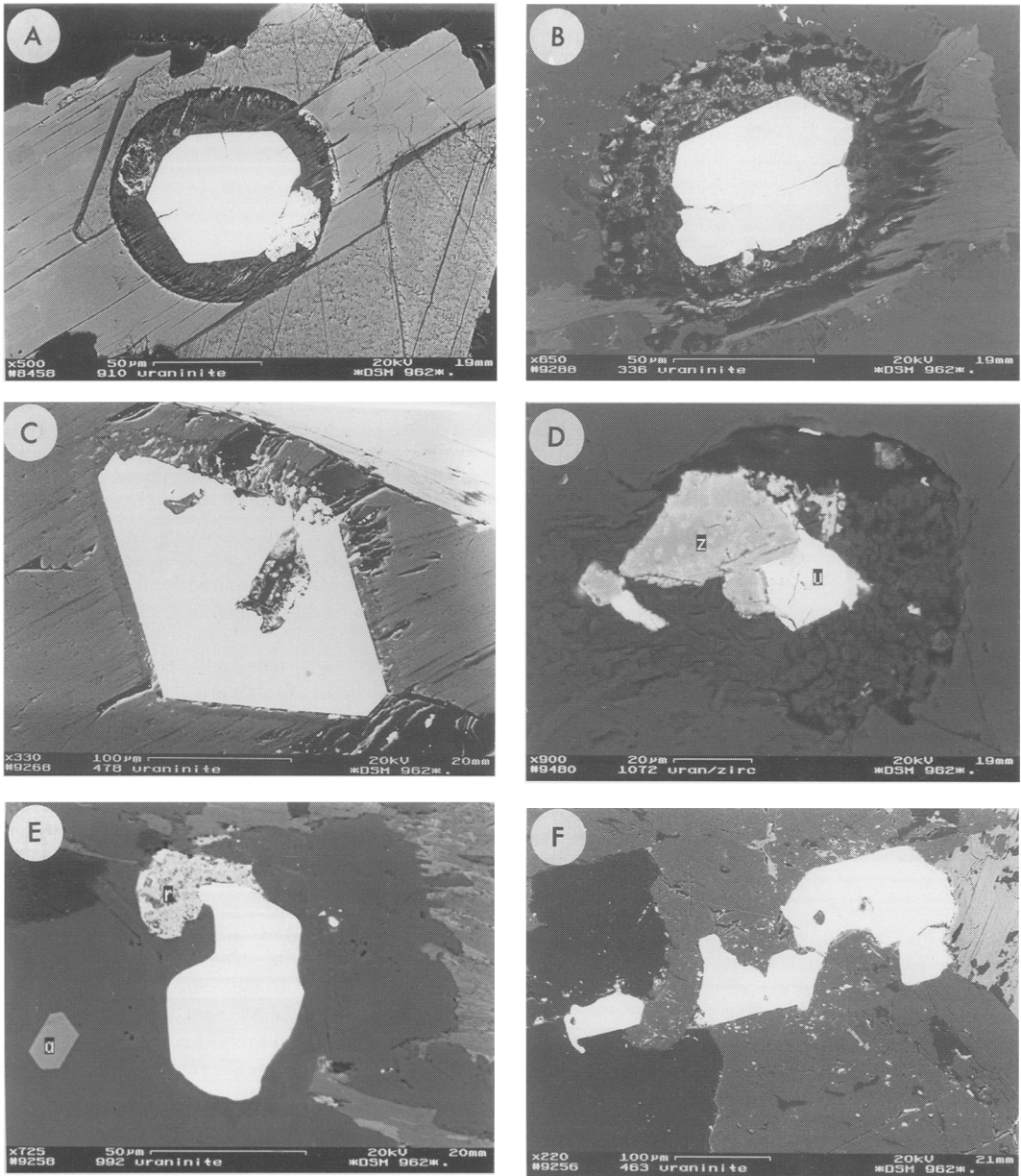


FIG. 2. Back-scattered scanning electron microscope images (BSE) of uraninites. [A] euhedral uraninite which has formed a spherical reaction rim due to alpha particle irradiation causing breakdown of the structure of the surrounding Li-Fe mica ('protolithionite'). [B] euhedral uraninite (Table 1, analysis 6), which has caused radiation damage in K-feldspar/biotite. [C] euhedral uraninite with small alteration rim in siderophyllite (Table 1, analysis 12). [D] subhedral uraninite associated with zircon (z). [E] anhedral uraninite associated with rutile (r) and included in plagioclase, a - apatite. [F] accumulation of rare large uraninite grains, which are partially broken and display localized dissolution (Table 1, analysis 9). Note that the BSE images were recorded with different beam current and different gain of the photomultiplier to optimize the resolution for each grain. Thus, areas of similar chemical composition do not show the same grey tone in the different BSE pictures.

nates over zoned grains. Compositional heterogeneity within single crystals reflects a systematic core to rim or patchy zonation. However, uraninite grains are usually too small to permit multiple analyses, and thus single-crystal scale variations in composition could only be determined rarely.

Chemical ages of uraninite

A chemical U-Th-total Pb age was calculated using the equation for the radioactive decay of U and Th (e.g. Rhede *et al.*, 1996, p. 248) for each plotted analysis. Single point ages, which refer to samples from the same group of granites, were then combined to determine an average age of uraninite from the biotite, two-mica, and S-type Li-mica granites, respectively. This procedure is justified because the ages of uraninites from granites belonging to one group are not distinguishable statistically which is consistent with the current knowledge that the radioactive ages of the respective plutons are similar.

The following chemical uraninite ages (1 Sigma standard deviation) were obtained: biotite granites, 321 ± 6 Ma ($n = 62$); Bergen two-mica granite, 320 ± 7 Ma ($n = 42$); S-type Li-mica granites, 314 ± 9 Ma ($n = 47$). They are in excellent agreement with isotopic U-Pb monazite and K-Ar mica ages, which cluster in a narrow interval between about 325 and 315 Ma (see Förster *et al.*, 1998), and support a magmatic to late-magmatic origin of uraninite in these granites as suggested from textural relations. It is further implied that the uraninite grains discussed in this paper did not suffer significant disturbances of their U-Th-Pb isotopic system and only contain very small amounts of non-radiogenic lead. The first major U mineralization event of economic importance in the Erzgebirge granites and their metamorphic country rocks took place at about 271 ± 7 Ma as implied by U-Pb ages of primary pitchblende from the Schlema-Alberoda vein-type deposit (Förster and Haack, 1995).

Mineral chemistry

Typical electron microprobe analyses of uraninite from the Erzgebirge granites are listed in Table 1. The analyses were selected to demonstrate the compositional variability of uraninite in terms of actinide and lanthanide element concentrations within the three groups of granites: biotite granites, two-mica granites, and S-type Li-mica

granites. In the various chemical variation diagrams (see Figs. 3–5 and 7), the individual granite groups are represented by uraninite from the following occurrences (see Fig. 1): biotite granites = Kirchberg, Burkersdorf, Schlema-Alberoda, Beierfeld, Niederbobritzsch; two-mica granites = Bergen; S-type Li-mica granites = Eibenstock, Tellerhäuser, Satzung, Pobershau.

Thorium

Thorium is substituted into the uraninite lattice in widely variable amounts. Both the concentration highs and lows of ThO₂ were determined in samples from biotite granites and amount to 11.0 and 0.4 wt.%, respectively (Fig. 3a). The Kirchberg biotite granite pluton contains exclusively Th-rich uraninite (thorian uraninite). In contrast, ThO₂ in grains from two-mica and S-type Li-mica granites is typically lower but variably ranging from 0.8 to 4.9 and 1.0 to 6.5 wt.%, respectively, and thus overlaps the concentrations of Th measured in uraninite from the other occurrences of biotite granite.

Yttrium and the heavy rare-earth elements

The content of Y₂O₃ varies from below the microprobe detection limit to 5.5 wt.% (Fig. 3b). Except of the Kirchberg granite, uraninite is poor in Y₂O₃, exhibiting concentrations usually less than 1 wt.%. Y₂O₃ variability is exceptionally large in uraninite from the Kirchberg granite, where contents between 0.5 and 5.5 wt.% were determined. Both the minimum and maximum concentrations refer to crystals that are included in quartz and localized in the same thin section made from an aplite. They also demonstrate extremes in the variation of HREE₂O₃ concentrations (here represented by the oxides of the even-numbered elements Gd, Dy, Er, and Yb), which are 0.5 and 3.5 wt.%, respectively (see Fig. 3b). Irrespective of the granite group, uraninite has commonly incorporated the HREE in total amounts less than 0.8 wt.%.

As expected, the contents of Y and the HREE in uraninite are positively correlated. On average, the mineral has incorporated these components in a ratio of 4:3. Larger deviations from this ratio are observed in the most Y-rich phases and indicate increasing abundances of non-analysed uneven-numbered HREE which also partly account for their lower analytical totals (e.g. Table 1, analysis 2). Accordingly, the total HREE₂O₃ concentration in most-Y enriched grains can be approximated to about 4.5 wt.%.

TABLE 1. Electron microprobe analyses of uraninite

Granite Sample	Biotite granites										Two-mica granites						S-type Li-mica granites					
	A-KIB 784-F feldspar	A-KIB 784-F quartz	KIB 785-F biotite	KIB 310-F quartz	KIB 310-F biotite	NBZ 336-F feldspar	BUR 992-F feldspar (r) 7#(core)	BUR 992-F feldspar (r) 8#(rim)	SLM 463-F feldspar	BRG 480-F quartz	BRG 480-F rutile	BRG 478-F feldspar	EIB 508-F quartz	EIB 320-F quartz	SZU 934-F Li-mica	EIB 1065-F quartz	EIB 320-F quartz	EIB 320-F quartz	TLH 965-F Li-mica			
Analysis	1	2	3	4	5	6	7#(core)	8#(rim)	9	10	11	12	13	14	15	16	17	18				
ThO ₂	11.04	9.67	9.20	8.61	5.59	4.49	5.17	0.88	0.39	4.82	2.13	0.79	6.55	4.31	3.79	2.41	1.61	1.00				
UO ₂	80.94	73.42	84.37	82.81	85.32	89.71	87.30	92.62	93.80	89.81	93.41	95.05	89.19	90.45	91.07	92.45	93.84	94.29				
Y ₂ O ₃	0.91	5.50	0.62	1.72	2.20	0.68	0.86	0.96	0.25	0.52	0.33	0.27	0.32	0.23	0.44	n.d.	n.d.	0.08				
Ce ₂ O ₃	n.d.	0.46	0.04	n.d.	0.22	0.02	0.11	0.08	0.06	0.08	0.08	0.00	n.d.	n.d.	0.04	n.d.	n.d.	0.07				
Nd ₂ O ₃	0.06	0.74	0.22	0.25	0.34	0.18	0.03	0.20	0.05	n.d.	0.14	0.06	n.d.	0.03	n.d.	0.04	0.06	0.01				
Sm ₂ O ₃	0.20	0.63	0.19	0.15	0.23	0.03	0.11	0.18	n.d.	0.02	n.d.	0.07	0.07	n.d.	n.d.	n.d.	0.11	n.d.				
Gd ₂ O ₃	0.35	1.12	0.24	0.23	0.56	0.10	0.12	0.25	n.d.	0.09	0.09	0.07	0.06	0.06	0.16	0.22	0.11	n.d.				
Dy ₂ O ₃	0.20	1.10	0.28	0.36	0.60	0.13	0.18	0.25	0.08	0.25	0.08	0.11	0.06	0.11	0.22	0.22	0.11	n.d.				
Er ₂ O ₃	0.23	0.76	0.05	0.30	0.44	0.18	0.06	0.19	0.11	n.d.	0.02	0.03	0.04	n.d.	n.d.	0.03	0.04	n.d.				
Yb ₂ O ₃	0.10	0.48	0.11	0.20	0.29	0.11	0.21	0.05	n.d.	0.02	n.d.	0.03	n.d.	n.d.	0.02	0.03	0.04	n.d.				
PbO	3.98	3.40	3.89	3.98	3.85	4.03	3.99	4.08	4.23	4.15	4.27	4.18	3.92	4.03	4.08	4.02	4.14	3.97				
Total	98.00	97.27	99.20	98.63	99.63	99.65	98.14	99.74	98.96	99.76	100.56	100.46	100.21	99.22	99.41	99.79	99.80	99.61				
Th	0.926	0.782	0.764	0.713	0.456	0.372	0.433	0.072	0.033	0.399	0.175	0.065	0.541	0.360	0.206	0.200	0.134	0.084				
U	6.640	5.807	6.852	6.708	6.806	7.255	7.164	7.453	7.694	7.280	7.529	7.634	7.201	7.389	7.548	7.488	7.643	7.684				
Y	0.178	1.040	0.120	0.334	0.420	0.131	0.168	0.185	0.050	0.100	0.064	0.051	0.062	0.045	0.021	0.084	0.015	0.010				
Ce	0.060	0.060	0.005	0.028	0.028	0.003	0.015	0.011	0.007	0.010	0.011	0.008	0.009	0.004	0.010	0.005	0.008	0.010				
Nd	0.007	0.093	0.029	0.033	0.044	0.023	0.004	0.026	0.006	0.003	0.019	0.008	0.009	0.004	0.010	0.005	0.008	0.002				
Sm	0.026	0.077	0.024	0.018	0.028	0.003	0.014	0.022	0.003	0.011	0.010	0.009	0.008	0.008	0.015	0.024	0.013	0.023				
Gd	0.042	0.131	0.029	0.028	0.066	0.013	0.015	0.030	0.010	0.030	0.010	0.009	0.007	0.013	0.025	0.025	0.013	0.023				
Dy	0.023	0.126	0.032	0.042	0.069	0.015	0.021	0.030	0.010	0.030	0.010	0.009	0.007	0.013	0.025	0.025	0.013	0.023				
Er	0.026	0.085	0.005	0.034	0.049	0.021	0.007	0.022	0.012	0.002	0.002	0.004	0.004	0.004	0.003	0.003	0.004	0.004				
Yb	0.011	0.052	0.012	0.022	0.032	0.013	0.024	0.006	0.006	0.002	0.002	0.004	0.004	0.004	0.003	0.003	0.004	0.004				
Pb	0.395	0.325	0.382	0.390	0.372	0.394	0.396	0.397	0.420	0.407	0.417	0.406	0.383	0.399	0.423	0.394	0.408	0.391				
Total	8.276	8.579	8.256	8.323	8.370	8.241	8.261	8.253	8.231	8.242	8.238	8.177	8.214	8.217	8.223	8.223	8.210	8.208				

Cations normalized to 16 oxygens. See Fig. 1 for explanations. n.d. — analysed but not detected. Blank spaces indicate elements not analysed. # — multiple analyses within zoned grains. (r) — intergrown with rutile. A — apfite

Analysis 6 additionally contains 0.04 wt.% Tb₂O₃ and 0.04 wt.% CaO; analysis 7 0.03wt.% Tb₂O₃; analysis 8 0.03 wt.% SiO₂, 0.04 wt.% Tb₂O₃, and 0.03 wt.% CaO; analysis 12 0.03 wt.% P₂O₅ and 0.09 wt.% SiO₂; analysis 16 0.02 wt.% Pr₂O₃, 0.04 wt.% Tb₂O₃, and 0.04 Ho₂O₃.

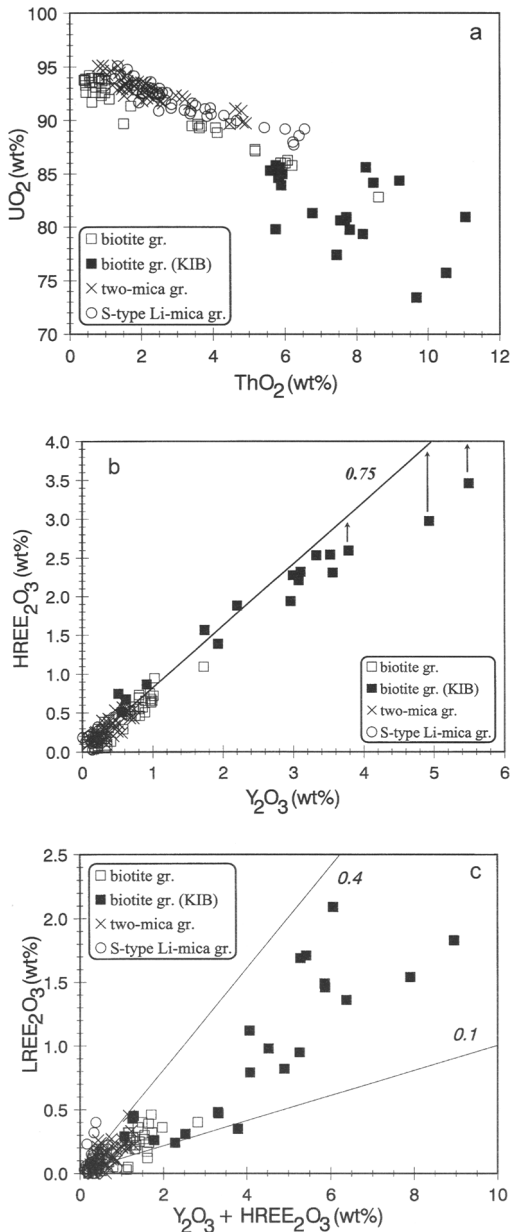


FIG. 3. Uraninite compositions (in wt.%) in terms of UO₂ vs. ThO₂ (a), HREE₂O₃ vs. Y₂O₃ (b), and LREE₂O₃ vs. the sum of HREE₂O₃ and Y₂O₃. KIB - Kirchberg.

Light rare-earth elements

The LREE₂O₃ contents (here as the sum of the oxides of the even-numbered elements Ce, Nd,

and Sm) in uraninite are generally much less than 0.5 wt.%, sometimes entirely below the microprobe sensitivity (Fig. 3c). Again, uraninite from the Kirchberg granite displays a contrasting behaviour with maximum LREE₂O₃ concentrations approaching 2.1 wt.%.

Other elements

In the vast majority of analyses, P, Si, Al, Ca and Fe were below the microprobe detection limits. If detected, P, Si, Al and Fe are present in concentrations less than 0.1 wt.%. CaO contents rarely approached 0.5 wt.%. In the unaltered uraninite crystals discussed in this paper, the maximum total contribution of these minor components amounts to 2.2 mol.%. Altered specimens, however, may contain up to 7 mol.%.

Compositional zonation

In the few cases where multiple analyses could be performed in compositionally heterogeneous crystals, systematic core-rim trends were observed frequently. Zonation, however, is commonly restricted to simple Th \rightleftharpoons U substitution and less developed with respect to the lanthanides and yttrium. The typical trend of decreasing Th and increasing U concentrations from the core to the rim is displayed by one single uraninite grain from the Burkersdorf biotite granite (Table 1, analyses 8 and 9). The same trend of evolution is also observed in crystals from two-mica granites and S-type Li-mica granites, with a maximum variability of ThO₂ content amounting 2.7 and 1.7 wt.%, respectively. In these granites, the grain-scale variations are similar to those recognized in the thin-section or even pluton scales.

Interelement correlations

In many uraninite grains, evolution of Th, Y, and REE concentrations displays the same trend (Fig. 4). Th-poor phases, which are characteristic of two-mica and S-type Li-mica granites, typically are similarly low in the abundances of lanthanides and yttrium. On the other hand, Th-rich uraninite may occur showing substantially depleted REE and Y contents, or vice versa. In uraninite from the Kirchberg massif, Th and the REE plus Y are both enriched and abundant in similar proportions. Uraninite shows a preference of Y and the HREE over the LREE, which are usually 4 to 10 times higher in total concentration (see Fig. 3c). Crystals, in which the LREE predominate, rarely exist.

Relations between accessory mineral and host rock compositions

In biotite granites, uraninite was discovered in weakly peraluminous rocks ($A/CNK = 1.05\text{--}1.14$) with varying degrees of differentiation containing 69 to 77 wt.% SiO_2 and 0.45 to 0.05 wt.% TiO_2 . It was identified in strongly peraluminous two-mica granites ($A/CNK = 1.15\text{--}1.27$), which cover intervals of 73 to 76 wt.% SiO_2 and 0.16 to 0.06 wt.% TiO_2 . Uraninite-bearing S-type Li-mica granites ($A/CNK = 1.17\text{--}1.33$) range in composition from 73 to 76 wt.% SiO_2 and 0.21 to 0.04 wt.% TiO_2 . Appearance of uraninite reflects the following minimum U concentrations in virtually unaltered samples: biotite granites = 9 ppm, two-mica granites = 12 ppm, and S-type Li-mica granites = 15 ppm.

Until now, little effort has spent on study of the relations between uraninite and whole-rock compositions worldwide. In this study, no clear correlations could be established with respect to Th (Fig. 5a). Both in Th-rich and -poor granites low- and high-Th uraninite may be observed. However, Th-rich rocks, as represented by the Kirchberg granite, appear to host uraninite with more enhanced levels of thorium. The situation is similar regarding yttrium. Y-enriched granites tend to host high-Y uraninite, although Y-poor varieties may also be present (Fig. 5b). This is well demonstrated by aplites from the Kirchberg pluton where uraninite representing both extremes in Y content occur within the same thin section and within the same type of host mineral (quartz).

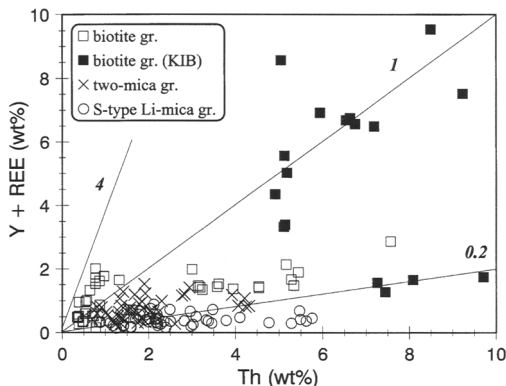


FIG. 4. Compositional variations (in wt.%) of $(Y + REE)$ and Th in uraninite from the different groups of peraluminous granites.

Uraninite with Y contents less than 1 wt.% may be present in rocks of widely variable Y concentration, whereas occurrence of uraninite higher in Y seems to be restricted to granites of more than 20 ppm Y. Although the rocks have a wide range in *LREE* content, the *LREE* abundance in uraninite remains nearly constant (Fig. 5c). A different situation is given in the Kirchberg granite where both parameters are negatively correlated.

Contribution of uraninite to the bulk-rock actinide and lanthanide budget

Uraninite contains an exceptional high percentage of the bulk-rock U content in thorite-free Erzgebirge granites. This is well demonstrated for example by a granite sample from the U-rich, Ca-poor Bergen two-mica granite massif (Fig. 6a). In this specific granite, mass-balance calculations imply that uraninite (and rare U micas) accounts for nearly 85 % of total U, even in the presence of monazite-(Ce) and cheralite-(Ce) (Förster, 1998a), xenotime (Förster, 1998b), and zircon, which all contain substantial amounts of U. On the other hand, the fraction of Th residing in uraninite is low ($< 5\%$). Its contribution to the lanthanide budget is negligible ($< 1\%$). Mass-balance calculations for the S-type Li-mica granites yield corresponding results.

Uraninite also constitutes the most important host for U in more evolved biotite granites containing abundant thorite, rich in uranium (up to 11 wt.% UO_2) (Fig. 6b). In a fine-grained intrusion within the Kirchberg massif, mass-balance calculations suggest that uraninite contains 75% of the total U budget. Compared to the Bergen two-mica granite sample, its contribution to the *REE*, Y and Th budgets is higher, though still usually less than 5%. U-rich thorite accounts for only about 10% of total U.

Discussion and concluding remarks

Not recognized in previous microscopic studies, electron microprobe investigations recognized uraninite as a common accessory in many Erzgebirge granites with typical U levels of >10 ppm.

UO_2 is always the essential structural component in uraninite, with the total proportion of U and radiogenic Pb between 71 and 99 mol.% (Fig. 7). It has incorporated Th, Y, and the *REE* in total amounts between 1 and 29 mol.% but

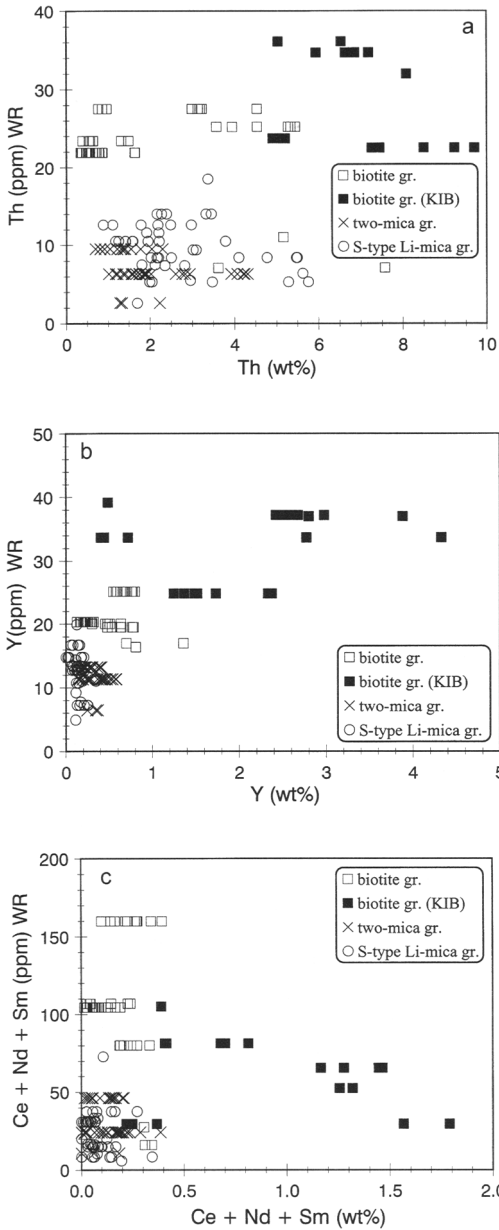


FIG. 5. Relations between the concentrations of Th (a), Y (b), and the *LREE* (c) in whole-rock (WR) and uraninite.

contains P, Si, Al, Fe, and Ca in subordinate amounts. In many cases, substitution of elements into the mineral lattice apparently took place via simple mechanisms, $U^{4+} \rightleftharpoons Th^{4+}$ and $U^{6+} \rightleftharpoons 2(Y, REE)^{3+}$.

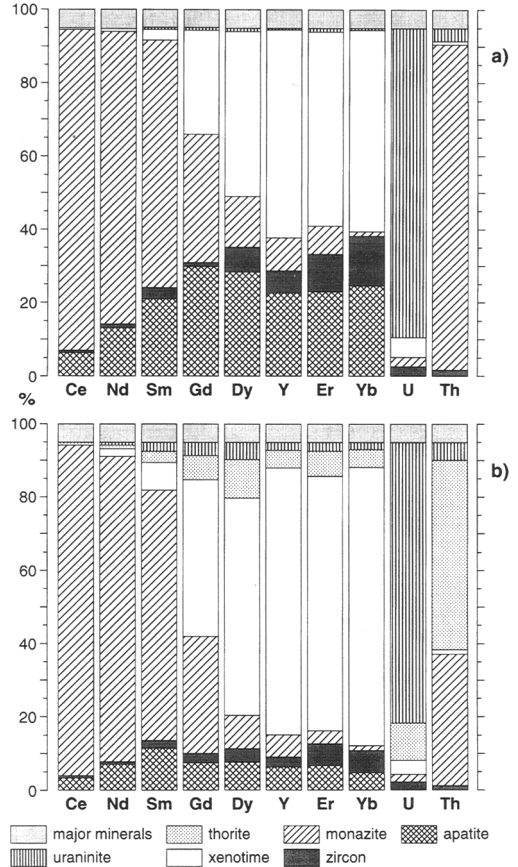


FIG. 6. Relative contribution of major and accessory minerals to the whole-rock lanthanide and actinide budget of a (a) medium-grained two-mica granite from the Bergen massif ($SiO_2 = 73.6$ wt.%, $TiO_2 = 0.158$ wt.%, $U = 14.5$ ppm, $Th = 9.5$ ppm, sum *LREE* = 65 ppm, sum *HREE* = 8.8 ppm, $Y = 13.2$ ppm) and a (b) fine-grained biotite granite from the Kirchberg massif ($SiO_2 = 77.1$ wt.%, $TiO_2 = 0.092$ wt.%, $U = 23$ ppm, $Th = 35$ ppm, sum *LREE* = 81 ppm, sum *HREE* = 21.9 ppm, $Y = 37$ ppm). For each element, its proportion contained in major minerals is approximated to 5%, following the results obtained by Bea (1996).

Established correlations between uraninite and host-granite compositions in the Erzgebirge correspond well with observations elsewhere. Strongly peraluminous leucogranites of S-type affinity represented by Variscan granites of SW England (Basham *et al.*, 1982; Jefferies, 1985; Charoy, 1986), Portugal (Pagel, 1982b), the

CHEMICAL COMPOSITION OF URANINITE

French Massif Central (Poty *et al.*, 1986), and the Harz Mts. in Germany (Ramberg granite; Leupolt, 1992), the Himalayan Manaslu granite (Cuney *et al.*, 1984) and the two-mica granites and S-type Li-mica granites from the Erzgebirge usually contain uraninite low in Th, Y, and the *REE*. In these granites, the ThO₂ content in uraninite rarely exceeds 6 wt.%. Atypically for this mode of environment, Bea (1996) reported extremely Th-rich uraninite from the Gredos granodiorite (17.5 wt.% ThO₂) and the Albuquerque U-rich leucogranite (11.2 wt.% ThO₂), both cordierite-bearing and located in Spain. The uraninite from the Tertiary low-Th Lundy granite (Thorpe *et al.*, 1989), SW England, may also be regarded as uncommonly high in ThO₂ (8.3 wt.%) for a highly peraluminous rock. These 'exceptional' uraninite crystals share the common feature of being very low in Y and the lanthanides. Consequently, Th is much more susceptible to variations than are the other constituents.

The compositions of uraninites from the Kirchberg granite closely resemble those of uraninites from metaluminous to weakly peraluminous biotite ± amphibole ± pyroxene granites which share the features of either I- or post-collisional A-type rocks and contain uranothorite ± sphene ± allanite and (in A-types) complex U-Ti-*REE*-Nb phases. Examples for those environments are the late-Caledonian granites of Scotland and western Ireland (Basham *et al.*, 1982; Feely *et al.*, 1989) and some late-Variscan granites from the Vosges, France (Pagel, 1982a), the Harz Mts., Germany (Brocken granite; Leupolt, 1992) and the Iberian Massif, Spain (Casillas *et al.*, 1995), which all have in common enhanced whole-rock contents of U (>10 ppm), Th (>25 ppm), Y (>30 ppm), and the *HREE*. Usually, uraninite from these granites contains ThO₂ in excess of 6 wt.% (up to 15 wt.%). Th-poor uraninite is occasionally reported (e.g. Basham *et al.*, 1982). Although rarely analysed, the lanthanide and yttrium contents are high as well. High Y₂O₃ concentrations are reported for uraninite from the Brocken granite (up to 4.4 wt.%; Leupolt, 1992) and the Las Naves del Marqués monzogranite in Spain (up to 8.2 wt.%; Casillas *et al.*, 1995). Remarkable enrichment in *LREE* (Ce₂O₃ + Nd₂O₃ + Sm₂O₃ = 1.85 wt.%) and *HREE* (Gd₂O₃ + Dy₂O₃ + Er₂O₃ + Yb₂O₃ = 2.9 wt.%) was observed in uraninite from the Caledonian Costello Murvey granite, western Ireland (Feely *et al.*, 1989).

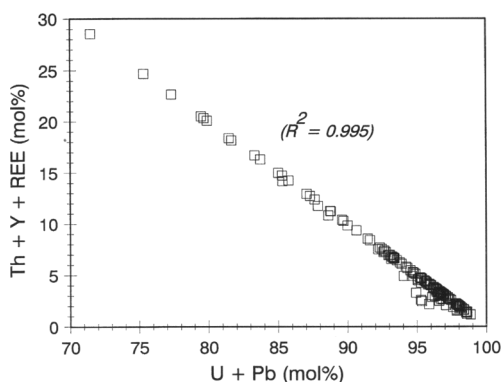


Fig. 7. Formula proportions (Th + Y + *REE*) vs. (U + Pb) in uraninite calculated on the basis of 16 oxygen atoms. R - correlation coefficient.

The total range of published EMP-produced concentrations (rounded to one decimal place) of Th, Y, and even-numbered *REE* in uraninite from peraluminous granites and granitic pegmatites is from zero up to the following values (in weight percent): ThO₂ = 17.1, Y₂O₃ = 8.2; Ce₂O₃ = 0.7, Nd₂O₃ = 0.9, Sm₂O₃ = 0.7, Gd₂O₃ = 1.1, Dy₂O₃ = 1.2, Er₂O₃ = 0.8. Uraninite grains from the Erzgebirge two-mica and S-type Li-mica granites are at the lower end and those from the Kirchberg pluton at the upper end of the concentration ranges.

Apparently, differences in the initial contents of Th, *LREE*, and (Y) in the granites have not caused the considerable diversity in uraninite compositions recorded within the group of biotite granites in the Erzgebirge (see Figs. 5a–c). Commonly, the high-Th content in uraninite is attributed to equilibrium crystallization with uranothorite (Poty *et al.*, 1986; Cuney and Friedrich, 1987). This appears to be a viable explanation for the compositional signatures of uraninite from the Kirchberg granite which indeed contain abundant uranothorite. However, uranothorite also occurs in those biotite granites which bear uraninite containing low concentrations of Th. Differences in the time of crystallization of uraninite is another factor that might have accounted for its variability in composition. Nevertheless, in the Kirchberg granite, the occurrence of the compositional extremes of uraninite in the same thin section and the same host mineral does not favour this interpretation. Furthermore, Th concentration in uraninite from the Manaslu granite does not correlate with the order of crystallization of its

mineral hosts (e.g. Cuney *et al.*, 1984). The sequence of crystallization of the uraninite-bearing minerals, however, is not always easy to recognize. These phases also may occur in different generations, which further complicates the situation.

Evolution of element contents during differentiation is not manifested in systematic changes in the actinide and lanthanide concentrations in uraninite from the granites representing discrete sub-phases within composite plutons. On the other hand, a decrease of Th from the core to the rim as observed in some uraninite grains in granites from all three groups, is consistent with the evolution of their host rocks. This is indicated by their decreasing Th content with progressive fractionation. It follows that host rock chemistry may exert control on uraninite composition, even if the exact mechanisms are not properly understood. Diffusion-controlled compositional gradients in the regions adjacent to growing major phases and the growing uraninite crystal itself, as invoked by Wark and Miller (1993), is one plausible mechanism to explain the observed irregularities in element concentrations on the grain-size scale. Although some uraninite grains are corroded, vacuolized, and rimmed by alteration minerals, no evidence exists that variations in Th concentration in uraninite crystals can be correlated with the intensity of alteration as suggested by Cuney *et al.* (1982), because fresh crystals may show the same pattern.

The high percentage of total U contained in uraninite from two-mica granites, S-type Li-mica granites as well as evolved thorite-bearing biotite granites supports the results obtained by Cuney and Friedrich (1987) that in fractionated low-Ca peraluminous granites between 70 and 90% of bulk-rock U content may reside in this mineral. The prominent role of xenotime as the main host for U (about 50–60%) in low-Ca peraluminous granites as recognized by Bea (1996) is not confirmed.

Acknowledgements

This work constitutes a part of the habilitation thesis of the author. I wish to thank D. Rhede and O. Appelt, Potsdam, for their continuous support during the many weeks of electron microprobe work. Dieter Rhede has also collaborated with the chemical age dating of radioactive accessory minerals. G. Tischendorf, Berlin, participated in many discussions on the genesis of U mineraliza-

tion in the Erzgebirge and provided valuable assistance in computing the mass-balance calculations. I.R. Basham and M. Feely are thanked for their constructive and careful reviews of the manuscript. XRF and ICP-MS whole-rock analyses were performed by R. Naumann and P. Dulski, Potsdam. I wish to acknowledge the assistance of Daniel Harlov, Potsdam, in improving a previous draft of this manuscript.

References

- Basham, I.R., Ball, T.K., Beddoe-Stephens, B. and Michie, U.McL. (1982) Uranium-bearing accessory minerals and granite fertility: II. Studies of granites from the British Isles. In: *Compte-rendu méthodes de prospection de l'uranium*; Symposium sur les méthodes de prospection de l'uranium — examen du programme AEN - AIEA de R & D. Organ. Econ. Coop. and Develop., Paris, 398–413.
- Bea, F. (1996) Residence of REE, Y, Th and U in granites and crustal protoliths; Implications for the chemistry of crustal melts. *J. Petrol.*, **37**, 521–52.
- Bowles, J.F.W. (1990) Age dating of individual grains of uraninite in rocks from electron microprobe analyses. *Chem. Geol.*, **83**, 47–53.
- Casillas, R., Nagy, G., Pantó, G., Brändle, J., and Fórizs, I. (1995) Occurrence of Th, U, Y, Zr, and REE-bearing accessory minerals in late-Variscan granitic rocks from the Sierra de Guadarrama (Spain). *Eur. J. Mineral.*, **7**, 989–1006.
- Charoy, B. (1986) The genesis of the Cornubian batholith (south-west England): the example of the Carnmenellis pluton. *J. Petrol.*, **27**, 571–604.
- Chauris, L., Laforêt, C. and Cotten, J. (1985) Uraninite dans le granite stanno-wolframifère de Montbelleux (Massif armoricain). *Bull. Minéral.*, **108**, 855–58.
- Chernyshev, I.V. and Golubev, V.N. (1996) The Strel'tsovskoe deposit, eastern Transbaikalia: isotope dating of mineralization in Russia's largest uranium deposit. *Geochem. Int.*, **34**, 834–46.
- Cocherie, A., Johan, V., Rossi, P. and Štemprok, M. (1991) Trace element variations and lanthanide tetrad effect studied in a Variscan lithium albite granite: Case of the Cinovec granite (Czechoslovakia). In *Source, Transport and Deposition of Metals* (M. Pagel and J.L. Leroy, eds.). Balkema, Rotterdam, 745–9.
- Cuney, M. and Friedrich, M. (1987) Physicochemical and crystal-chemical controls on accessory mineral paragenesis in granitoids: implications for uranium metallogenesis. *Bull. Minéral.*, **110**, 235–47.
- Cuney, M., Le Fort, P. and Wang, Z.X. (1984) Uranium and thorium geochemistry and mineralogy in the Manaslu leucogranite (Nepal, Himalaya). In *Geology*

- of *Granites and their Metallogenic Relations* (Xu Kewqin and Tu Guangchi, eds.), Proc. of the Int. Symp., Nanjing, China, Oct. 26–30, 1982, 853–73.
- Drake, M.J. and Weill, D.F. (1972) New rare earth elements standards for electron microprobe analysis. *Chem. Geol.*, **10**, 179–81.
- Fayek, M., Janeczek, J. and Ewing, R.C. (1997) Mineral chemistry and oxygen isotopic analyses of uraninite, pitchblende and uranium alteration minerals from the Cigar Lake deposit, Saskatchewan, Canada. *Applied Geochem.*, **12**, 549–65.
- Feely, M., McCabe, E. and Williams, C.T. (1989) U-, Th- and REE-bearing accessory minerals in a high heat production leucogranite within the Galway Granite, western Ireland. *Trans. Inst. Mining Metall.*, **98**, B27–32.
- Foord, E., Korzeb, S.L., Lichte, F.E. and Fitzpatrick, J.J. (1997) Additional studies on mixed uranyl oxide-hydroxide hydrate alteration products of uraninite from the Palermo and Ruggles granitic pegmatites, Grafton County, New Hampshire. *Canad. Mineral.*, **35**, 145–51.
- Förster, B. and Haack, U. (1995) U/Pb-Datierungen von Pechblenden und die hydrothermale Entwicklung der U-Lagerstätte Aue-Niederschlema (Erzgebirge). *Z. geol. Wiss.*, **23**, 581–88.
- Förster, H.-J. (1998a) The chemical composition of REE-Y-Th-U-rich accessory minerals from the Erzgebirge-Fichtelgebirge region, Germany. Part I: The monazite-(Ce) - brabantite solid solution series. *Amer. Mineral.*, **83**, 259–72.
- Förster, H.-J. (1998b) The chemical composition of REE-Y-Th-U-rich accessory minerals from peraluminous granites of the Erzgebirge-Fichtelgebirge region, Germany. Part II: Xenotime. *Amer. Mineral.*, **86**, 1302–15.
- Förster, H.-J. and Tischendorf, G. (1994) The western Erzgebirge-Vogtland granites: Implications to the Hercynian magmatism in the Erzgebirge-Fichtelgebirge anticlinorium. In *Metallogeny of Collisional Orogens* (R. Seltmann, H. Kämpf and P. Möller, eds.), Czech Geol. Surv., Prague. 35–48.
- Förster, H.-J., Seltmann, R. and Tischendorf, G. (1995) High-fluorine, low-phosphorus A-type (post-collision) silicic magmatism in the Erzgebirge. *Terra Nostra*, No. 7, 32–35.
- Förster, H.-J., Tischendorf, G., Seltmann, R. and Gottesmann, B. (1998) Die variszischen Granite des Erzgebirges: neue Aspekte aus stofflicher Sicht. *Z. geol. Wiss.*, **26**, 31–60.
- Friedrich, M.H. and Cuney, M. (1989) Uranium enrichment processes in peraluminous magmatism. In *Uranium Deposits in Magmatic and Metamorphic Rocks*, IAEA-TC-571/2, International Atomic Energy Agency, Vienna, 11–35.
- Fryer, B.J. and Taylor, R.P. (1987) Rare-earth element distributions in uraninites: implications for ore genesis. *Chem. Geol.*, **63**, 101–8.
- Hidaka, H., Holliger, P., Shimizu, H. and Masuda, A. (1992) Lanthanide tetrad effect observed in the Oklo and ordinary uraninites and its implication for their formation processes. *Geochem. J.*, **26**, 337–46.
- Jackson, S.E., Longerich, H.P., Dunning, G.R. and Fryer, B.J. (1992) The application of laser-ablation microprobe - inductively coupled plasma - mass spectrometry (LAM-ICP-MS) to in situ trace-element determinations in minerals. *Canad. Mineral.*, **30**, 1049–64.
- Jarosewich, E. and Boatner, L.A. (1991) Rare-earth element reference samples for electron microprobe analysis. *Geostandards Newsletter*, **15**, 397–9.
- Jefferies, N.L. (1985) Uraninite within the Carnmenellis pluton, Cornwall. In *High Heat Production (HHP) Granites, Hydrothermal Circulation and Ore Genesis* (Ch. Halls, ed.), 163–168. The Institution of Mining and Metallurgy, London.
- Kotzer, T.G. and Kyser, T.K. (1993) O, U, and Pb isotopic and chemical variations in uraninite: Implications for determining the temporal and fluid history of ancient terrains. *Amer. Mineral.*, **78**, 1262–74.
- Kucha, H., Lis, J. and Sylwestrzak, H. (1986) The application of the electron microprobe to dating of U-Th-Pb uraninite from the Karkonosze granites (Lower Silesia). *Mineral. Polonica*, **17**, 43–7.
- Lange, G., Mühlstedt, P., Freyhoff, G. and Schröder, D. (1991) Der Uranerzbergbau in Thüringen und Sachsen - ein geologisch-bergmännischer Überblick. *Erzmetall*, **44**, 162–71.
- Leupolt, L. (1992) *Radiometrischer Vergleich der Uran- und Thoriumgehalte in magmatischen Gesteinen sowie den darin akzessorisch auftretenden Mineralen des Harzes und der Buur-Region (Somalia)*. Thesis, Technische Universität Berlin.
- Pagel, M. (1982a) The mineralogy and geochemistry of uranium, thorium, and rare-earth elements in two radioactive granites of the Vosges, France. *Mineral. Mag.*, **46**, 149–61.
- Pagel, M. (1982b) Succession paragénetiques et teneurs en uranium des minéraux accessoires dans les roches granitiques: guides pour la recherche des granites favorables à la présence de gisements d'uranium. In: *Compte-rendu méthodes de prospection de l'uranium*; Symposium sur les méthodes de prospection de l'uranium — examen dur programme AEN - AIEA de R & D. Organ. Econ. Coop. and Develop., Paris, 445–56.
- Parslow, G.R., Brandstätter, F., Kurat, K. and Thomas, D.J. (1985) Chemical ages and mobility of U and Th in anatectites of the Creek Lake Zone, Saskatchewan. *Canad. Mineral.*, **23**, 543–51.
- Poty, B., Leroy, J., Cathelineau, M., Cuney, M.,

- Friedrich, M., Lespinasse, M. and Turpin, L. (1986) Uranium deposits spatially related to granites in the French part of the Hercynian orogen. In *Vein Type Uranium Deposits*, IAEA-TC-361, International Atomic Energy Agency, Vienna, 215–46.
- Rhede, D., Wendt, I. and Förster, H.-J. (1996) A three-dimensional method for calculating independent chemical U/Pb- and Th/Pb-ages of accessory minerals. *Chem. Geol.*, **130**, 247–53.
- Rimsaite, J. (1989) Genetic significance of inclusions and fracture fillings in magmatic and metamorphic rocks from selected Canadian uranium occurrences. In *Uranium Deposits in Magmatic and Metamorphic Rocks*, IAEA-TC-571/11. International Atomic Energy Agency, Vienna, 167–88.
- Rong, J., Han, Z. and Xia, Y. (1989) Uranium metallogenesis of coarse grained granite in Area H, China. In *Uranium Deposits in Magmatic and Metamorphic Rocks*, IAEA-TC-571/7, International Atomic Energy Agency, Vienna, 93–113.
- Snetsinger, K.G. and Polkowski, G. (1977) Rare accessory uraninite in a Sierran granite. *Amer. Mineral.*, **62**, 587–8.
- Thomas, R. (1988) *Untersuchungen von Schmelzeinschlüssen und ihre Anwendung zur Lösung lagerstättengeologischer und petrologischer Problemstellungen*. Habilitation Thesis, Bergakademie Freiberg.
- Thorpe, R.S., Tindle, A.G. and Gledhill, A. (1990) The petrology and origin of the Tertiary Lundy granite (Bristol Channel, UK). *J. Petrol.*, **31**, 1379–406.
- Tischendorf, G. (1989) Silicic Magmatism and Metallogenesis of the Erzgebirge. *Veröff. Zentralinst. Physik Erde Potsdam*, **107**, 316 pp.
- Tischendorf, G. and Förster, H.-J. (1994) Hercynian granite magmatism and related metallogenesis in the Erzgebirge: A status report. In *Mineral Deposits of the Erzgebirge/Krušné hory (Germany/Czech Republic)* (Kv. Gehlen and D.D. Klemm, eds.). Monograph Series on Mineral Deposits, **31**, 5–23.
- Wark, D.A. and Miller, C.F. (1993) Accessory mineral behavior during differentiation of a granite suite: monazite, xenotime, and zircon in the Sweetwater Wash pluton, southeastern California, U.S.A. *Chem. Geol.*, **110**, 49–67.
- Yudintsev, S.V. and Simonova, L.I. (1992) Radiochemistry of tin-bearing lithium-fluorine granites. *Geochem. Intern.*, **29**, 48–55.

[Manuscript received 1 April 1998:
revised 10 July 1998]